

Pt(II) Diimine Complexes Bearing Carbazolyl-capped Acetylide Ligands: Synthesis, Tunable Photophysics and Nonlinear Absorption

Rui Liu,^{a,b} Hongbin Chen,^a Jin Chang,^{a,c} Yuhao Li,^b Hongjun Zhu^{a,*} and Wenfang Sun^{b,*}

^a*Department of Applied Chemistry, College of Science, Nanjing University of Technology, Nanjing 210009, P. R. China.* ^b*Department of Chemistry and Biochemistry, North Dakota State University, Fargo, North Dakota 58108-6050, USA.* ^c*Discipline of Chemistry, Queensland University of Technology, 2 George St., Brisbane, 4000, Australia*

* Corresponding author. Phone: 701-231-6254. Fax: 701-231-8831. E-mail: Wenfang.Sun@ndsu.edu (W. Sun)

* Corresponding author. Phone: +86-25-83172358. Fax: +86-25-83587428. E-mail: zhuhj@njut.edu.cn (H. Zhu)

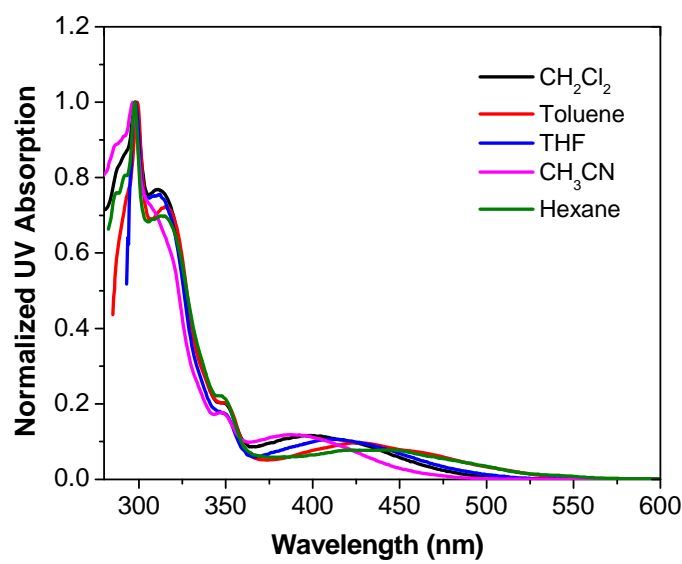


Figure S1. Normalized UV-vis absorption spectra of **Pt-1** in different solvents. $A_{436} = 0.08$

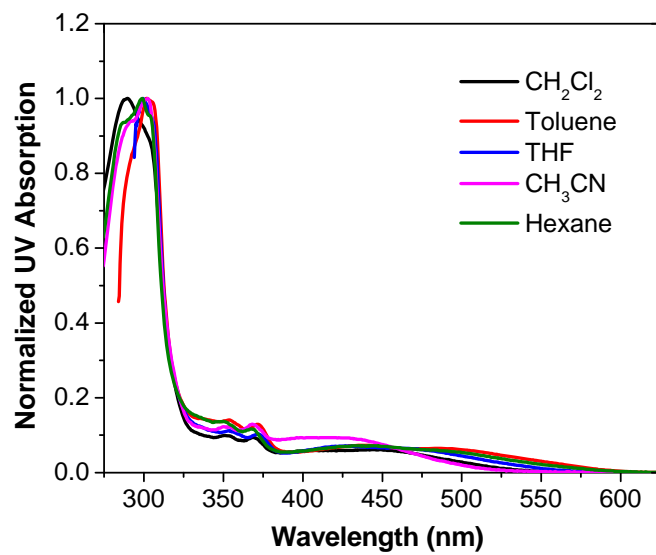


Figure S2. Normalized UV-vis absorption spectra of **Pt-2** in different solvents. $A_{436} = 0.08$

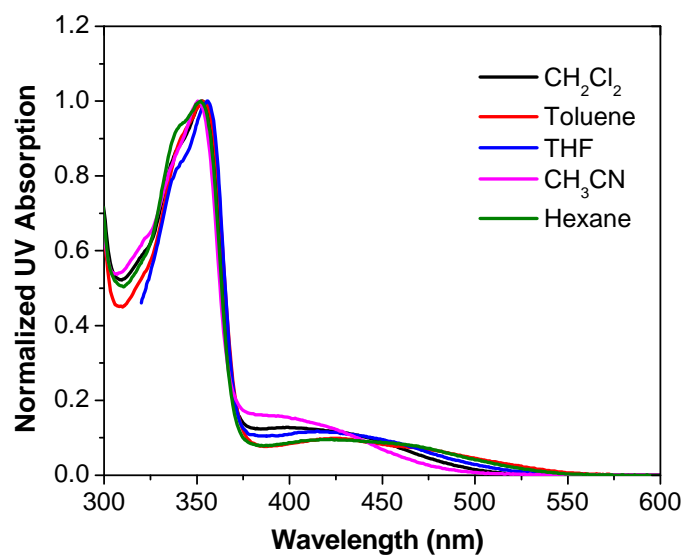


Figure S3. Normalized UV-vis absorption spectra of **Pt-4** in different solvents. $A_{436} = 0.08$

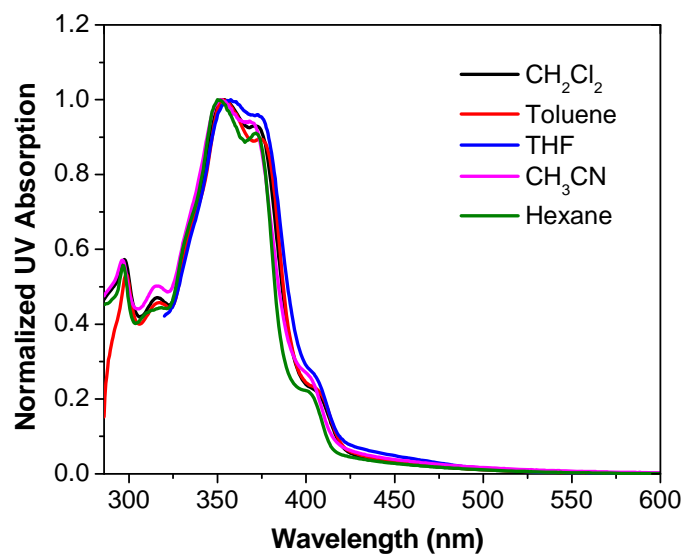


Figure S4. Normalized UV-vis absorption spectra of **Pt-5** in different solvents. $A_{436} = 0.08$

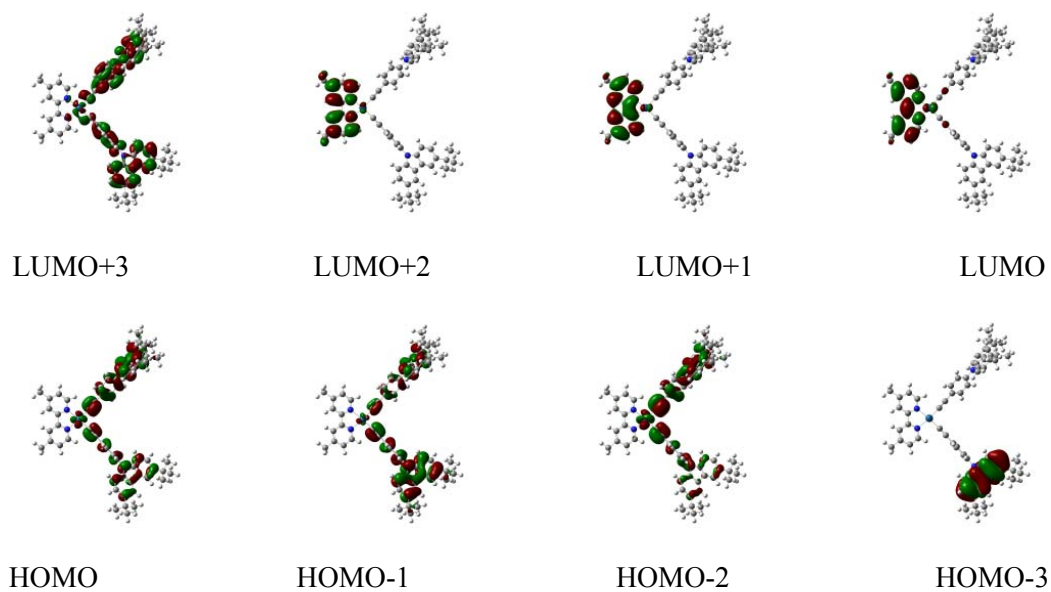


Figure S5. Contour plots of the four highest occupied molecular orbitals (HOMOs) and four lowest unoccupied molecular orbitals (LUMOs) of complex **Pt-1**.

Table S1. Excitation energies (eV), wavelengths (nm), oscillator strengths, dominant contributing configuration, and the associated configuration coefficient of five low-lying electronic states of complex **Pt-1** obtained at the CAM-B3LYP level of theory.

S_n	Excitation energy		f	Active orbital pair of dominant configuration	Configuration coefficient
	eV	nm			
1	2.77	448	0.0430	HOMO → LUMO	0.54
2	2.97	417	0.0369	HOMO-5 → LUMO	0.48
3	3.21	387	0.1490	HOMO-6 → LUMO	0.62
4	3.41	364	0.0027	HOMO-10 → LUMO	0.69
5	3.48	357	0.0633	HOMO-7 → LUMO	0.59
6	3.86	322	0.0025	HOMO-2 → LUMO	0.50
7	3.99	310	0.0000	HOMO-5 → LUMO	0.46
8	4.04	307	0.0343	HOMO → LUMO+1	0.52
9	4.17	297	0.0063	HOMO-1 → LUMO+1	0.38
10	4.23	293	0.3777	HOMO → LUMO+4	0.42

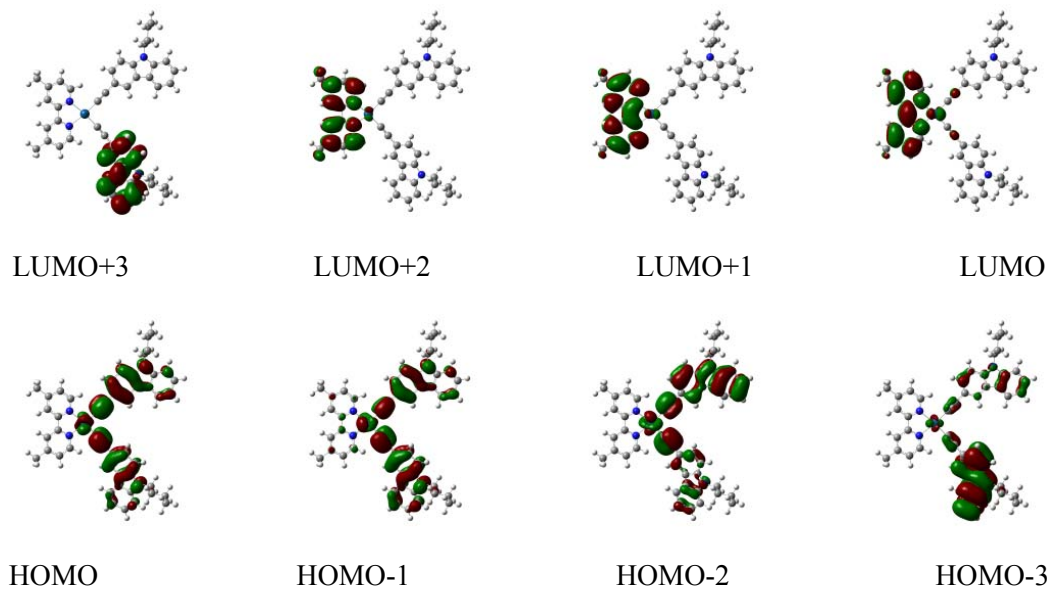


Figure S6. Contour plots of the four highest occupied molecular orbitals (HOMOs) and four lowest unoccupied molecular orbitals (LUMOs) of complex **Pt-2**.

Table S2. Excitation energies (eV), wavelengths (nm), oscillator strengths, dominant contributing configuration, and the associated configuration coefficient of five low-lying electronic states of complex **Pt-2** obtained at the CAM-B3LYP level of theory.

S_n	Excitation energy		f	Active orbital pair of dominant configuration	Configuration coefficient
	eV	nm			
1	2.44	509	0.0630	HOMO → LUMO	0.66
2	2.68	463	0.1914	HOMO-1 → LUMO	0.65
3	3.07	403	0.0296	HOMO-4 → LUMO	0.68
4	3.30	376	0.0020	HOMO-8 → LUMO	0.70
5	3.68	337	0.0120	HOMO-5 → LUMO	0.50
6	3.70	335	0.0283	HOMO → LUMO+1	0.60
7	3.82	325	0.0013	HOMO-1 → LUMO+1	0.52
8	4.04	307	0.0055	HOMO-2 → LUMO	0.45
9	4.05	306	0.1925	HOMO → LUMO+2	0.49
10	4.08	304	0.0765	HOMO-1 → LUMO+3	0.36

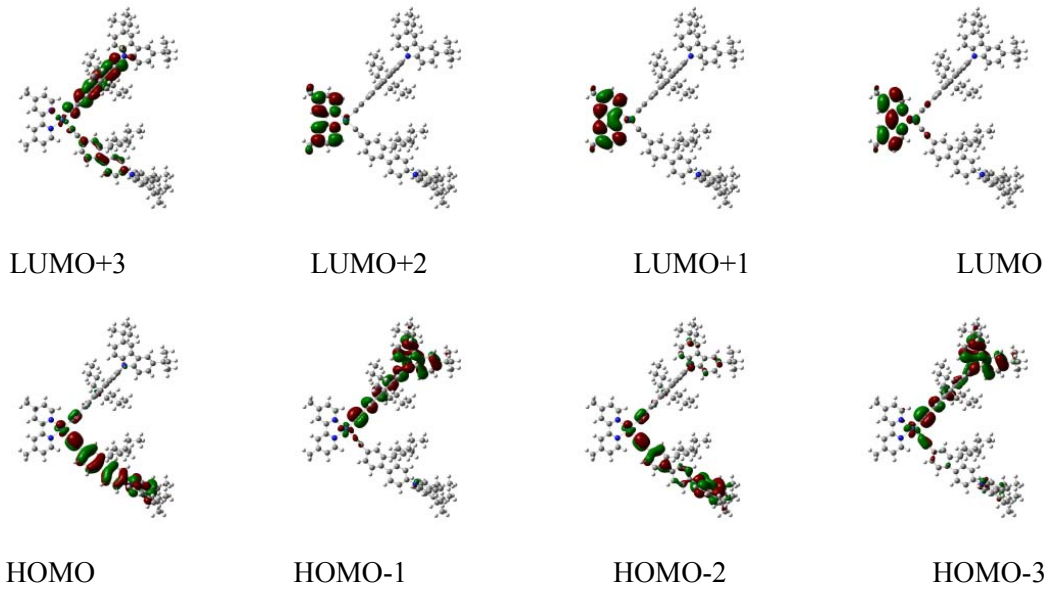


Figure S7. Contour plots of the four highest occupied molecular orbitals (HOMOs) and four lowest unoccupied molecular orbitals (LUMOs) of complex **Pt-4**.

Table S3. Excitation energies (eV), wavelengths (nm), oscillator strengths, dominant contributing configuration, and the associated configuration coefficient of five low-lying electronic states of complex **Pt-4** obtained at the CAM-B3LYP level of theory.

S_n	Excitation energy		f	Active orbital pair of dominant configuration	Configuration coefficient
	eV	nm			
1	2.67	465	0.1406	HOMO → LUMO	0.57
2	2.84	437	0.0269	HOMO-1 → LUMO	0.52
3	3.18	390	0.2199	HOMO-6 → LUMO	0.67
4	3.38	366	0.0019	HOMO-11 → LUMO	0.68
5	3.58	346	0.0168	HOMO-7 → LUMO	0.62
6	3.86	321	1.0076	HOMO → LUMO+1	0.39
7	3.92	316	0.2686	HOMO-2 → LUMO	0.32
8	3.98	311	0.2178	HOMO-2 → LUMO	0.42
9	4.04	307	0.0512	HOMO-1 → LUMO+1	0.35
10	4.07	305	1.4503	HOMO-1 → LUMO+3	0.48

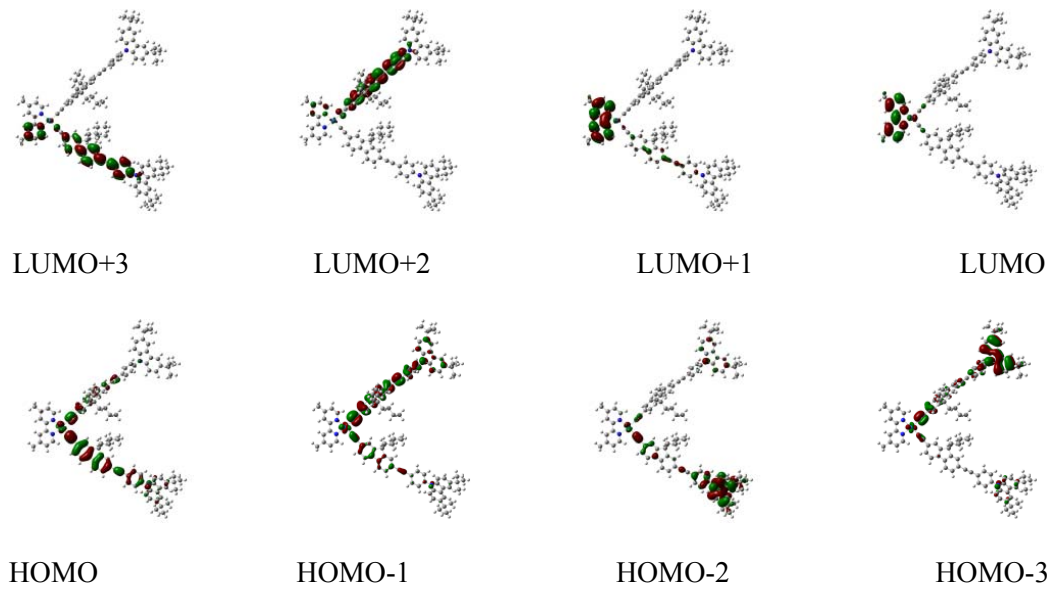


Figure S8. Contour plots of the four highest occupied molecular orbitals (HOMOs) and four lowest unoccupied molecular orbitals (LUMOs) of complex **Pt-5**.

Table S4. Excitation energies (eV), wavelengths (nm), oscillator strengths, dominant contributing configuration, and the associated configuration coefficient of five low-lying electronic states of complex **Pt-5** obtained at the CAM-B3LYP level of theory.

S_n	Excitation energy		f	Active orbital pair of dominant configuration	Configuration coefficient
	eV	nm			
1	2.64	469	0.1761	HOMO → LUMO	0.60
2	2.82	440	0.1585	HOMO-1 → LUMO	0.57
3	3.18	390	0.2722	HOMO-6 → LUMO	0.52
4	3.39	366	0.0032	HOMO-12 → LUMO	0.69
5	3.50	354	1.9495	HOMO → LUMO+3	0.39
6	3.64	341	2.6562	HOMO-1 → LUMO+2	0.39
7	3.65	339	0.3923	HOMO-9 → LUMO	0.49
8	3.90	318	0.0104	HOMO → LUMO+1	0.50
9	4.02	308	0.0008	HOMO-1 → LUMO+1	0.48
10	4.03	307	0.0100	HOMO-2 → LUMO	0.39

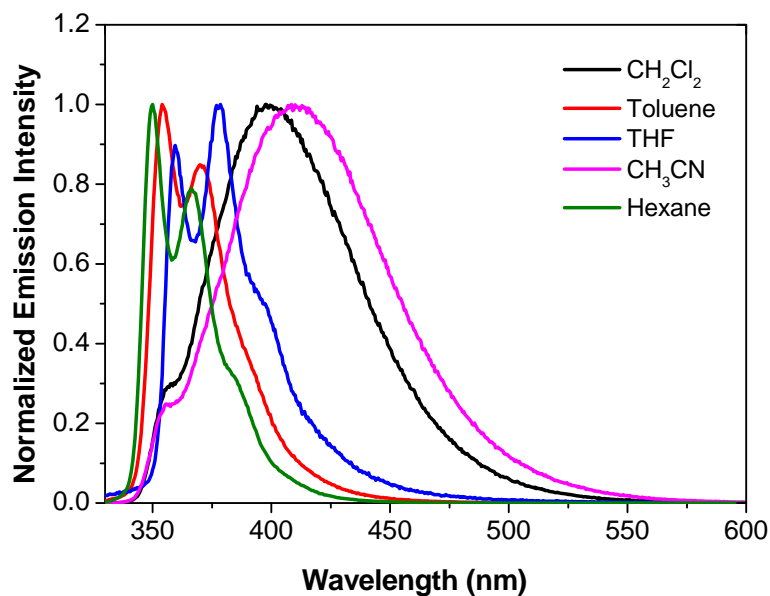


Figure S9. Normalized emission spectra of **L-1** in different solvents at room temperature,
 $\lambda_{\text{ex}} = 340 \text{ nm}$.

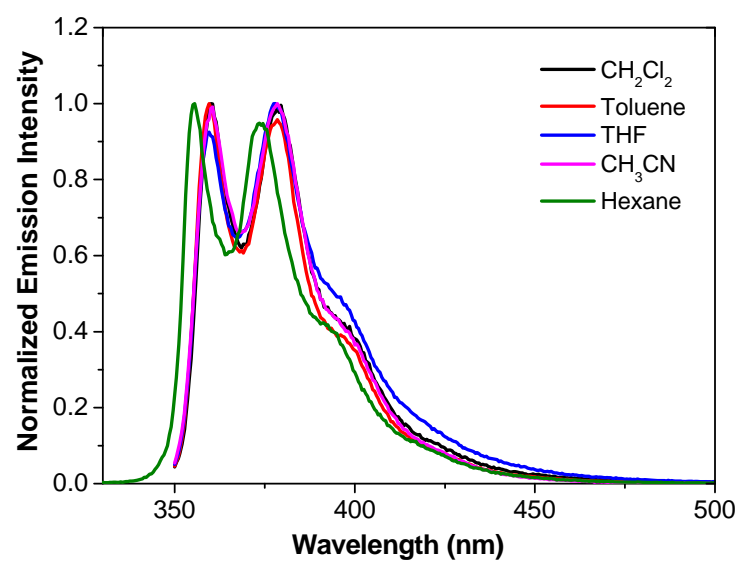


Figure S10. Normalized emission spectra of **L-2** in different solvents at room temperature, $\lambda_{\text{ex}} = 340 \text{ nm}$.

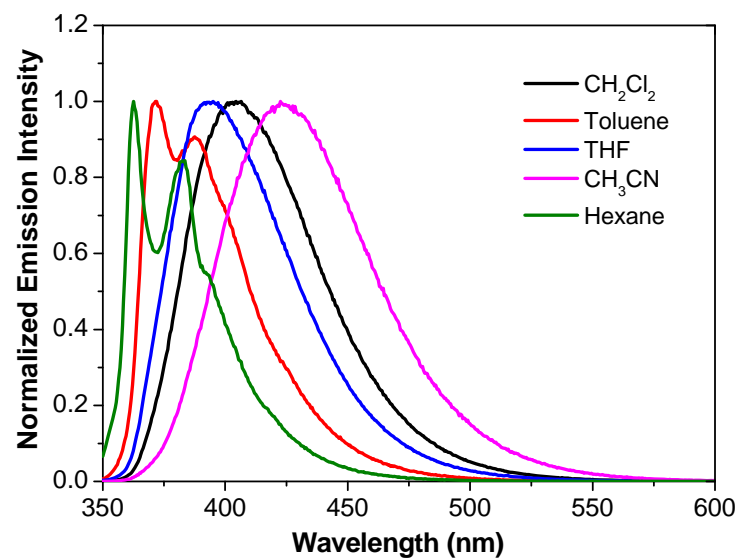


Figure S11. Normalized emission spectra of **L-3** in different solvents at room temperature, $\lambda_{\text{ex}} = 340$ nm.

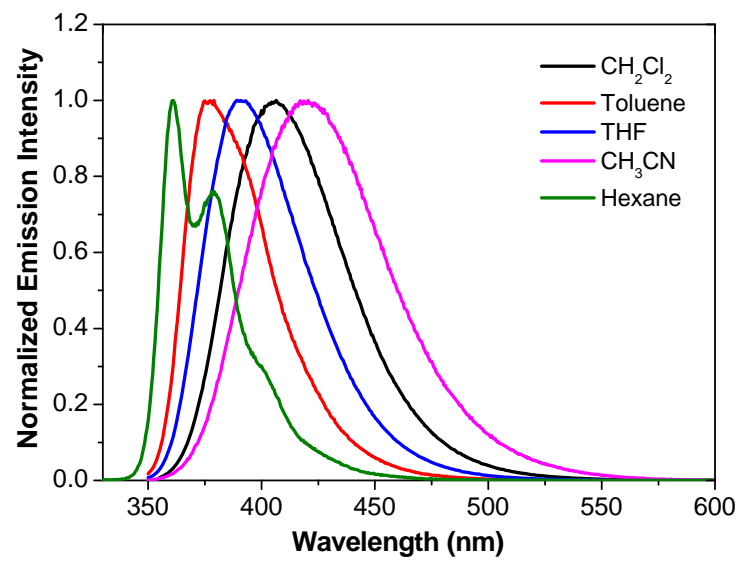


Figure S12. Normalized emission spectra of **L-4** in different solvents at room temperature, $\lambda_{\text{ex}} = 340$ nm.

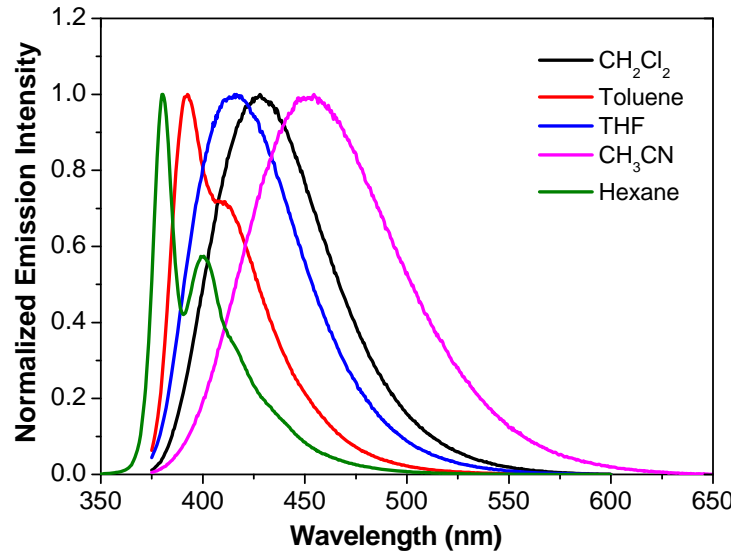


Figure S13. Normalized emission spectra of **L-5** in different solvents at room temperature, $\lambda_{\text{ex}} = 340$ nm.

Table S5. Emission energy and quantum yield of ligands **L-1 – L-5** in different solvents at room temperature

	$\lambda_{\text{em}} / \text{nm} (\Phi_{\text{em}}^{\text{[a]}})$				
	CH ₃ CN	CH ₂ Cl ₂	THF	Toluene	Hexane
L-1	410 (0.30)	399 (0.37)	379 (0.25)	354 (0.35)	350 (0.22)
L-2	378 (0.23)	379 (0.19)	378 (0.30)	359 (0.31)	356 (0.23)
L-3	423 (0.67)	405 (0.64)	395 (0.56)	372 (0.73)	362 (0.44)
L-4	419 (0.75)	407 (0.73)	391 (0.71)	377 (0.92)	361 (0.75)
L-5	452 (0.68)	428 (0.96)	417 (0.94)	393 (0.95)	381 (0.93)

[a] A aqueous solution of quinine sulfate ($\Phi_{\text{em}}=0.546$, excited at 365 nm) was used as the reference.

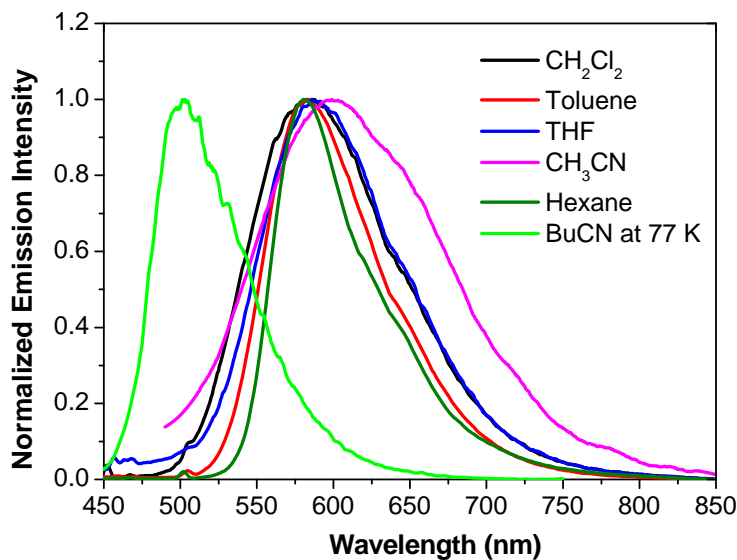


Figure S14. Normalized emission spectra of **Pt-1** in different solvents at room temperature and in BuCN glassy matrix at 77 K, $\lambda_{\text{ex}} = 436$ nm.

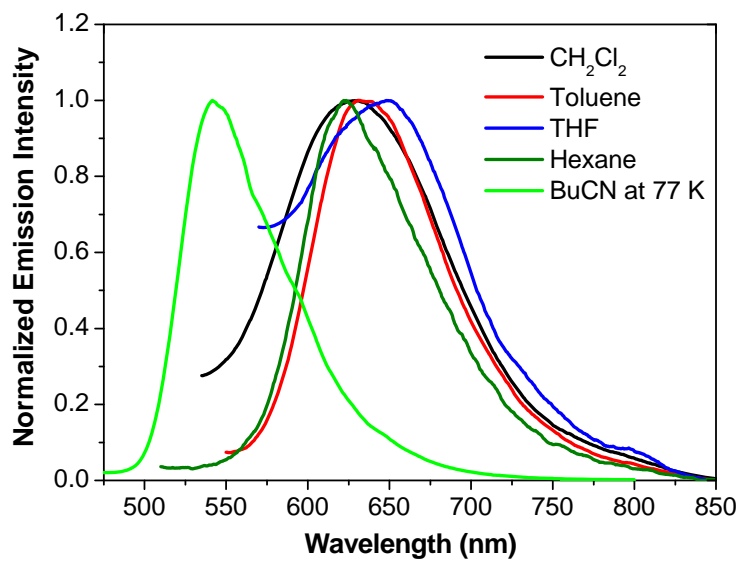


Figure S15. Normalized emission spectra of **Pt-2** in different solvents at room temperature and in BuCN glassy matrix at 77 K, $\lambda_{\text{ex}} = 436$ nm.

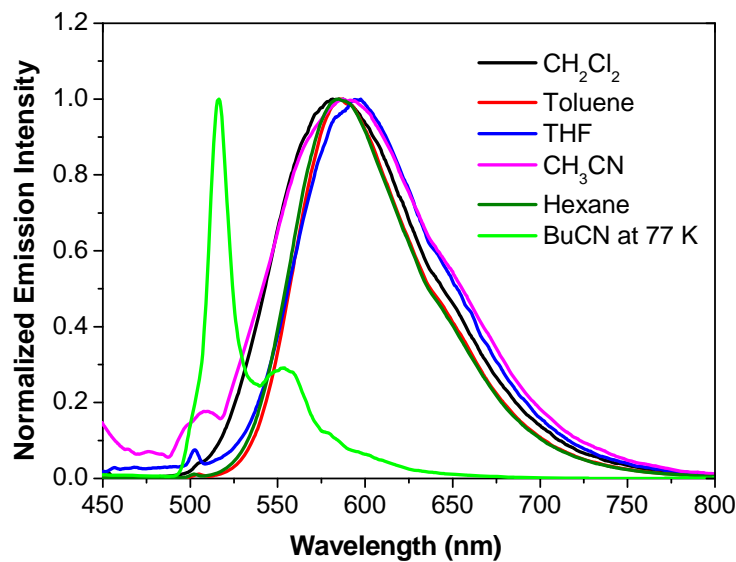


Figure S16. Normalized emission spectra of **Pt-4** in different solvents at room temperature and in BuCN glassy matrix at 77 K, $\lambda_{\text{ex}} = 436$ nm.

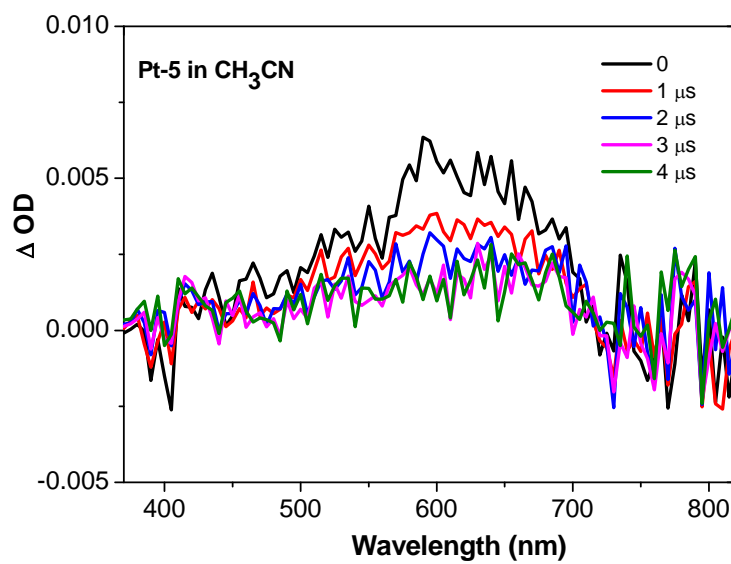


Figure S17. Nanosecond time-resolved transient absorption spectra of **Pt-5** in CH₃CN, $\lambda_{\text{ex}} = 355$ nm, $A = 0.4$ at 355 nm in a 1-cm cuvette. $\tau_{\text{TA}} = 2.73 \mu\text{s}$ at 590 nm.